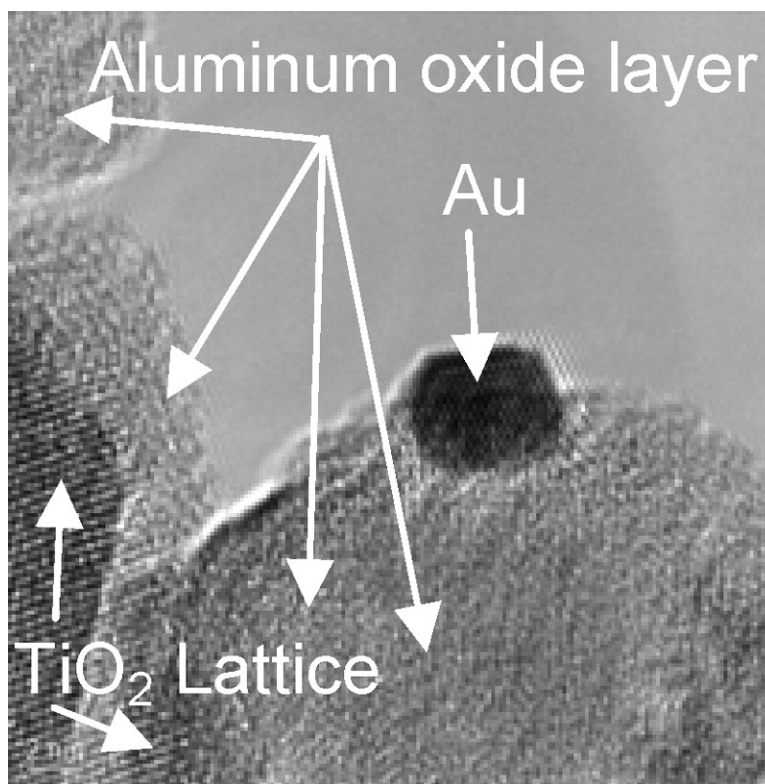


## Ultrastable Au Nanocatalyst Supported on Surface-Modified TiO Nanocrystals

Wenfu Yan, Shannon M. Mahurin, Zhengwei Pan, Steven H. Overbury, and Sheng Dai

*J. Am. Chem. Soc.*, **2005**, 127 (30), 10480-10481 • DOI: 10.1021/ja053191k • Publication Date (Web): 09 July 2005

Downloaded from <http://pubs.acs.org> on March 25, 2009



### More About This Article

Additional resources and features associated with this article are available within the HTML version:

- Supporting Information
- Links to the 11 articles that cite this article, as of the time of this article download
- Access to high resolution figures
- Links to articles and content related to this article
- Copyright permission to reproduce figures and/or text from this article



[View the Full Text HTML](#)



## Ultrastable Au Nanocatalyst Supported on Surface-Modified TiO<sub>2</sub> Nanocrystals

Wenfu Yan, Shannon M. Mahurin, Zhengwei Pan, Steven H. Overbury, and Sheng Dai\*

Chemical Sciences Division, Oak Ridge National Laboratory, Oak Ridge, Tennessee 37831

Received May 16, 2005; E-mail: dais@ornl.gov

Supported Au nanocatalysts have very high activities in some important industrial reactions, including oxidation of CO and hydrocarbons, water-gas-shift (WGS) reaction, H<sub>2</sub>O<sub>2</sub> production from H<sub>2</sub> and O<sub>2</sub>, removal of CO from hydrogen streams, and selective epoxidation.<sup>1–13</sup> Most of these reactions are currently catalyzed by platinum-group metals. Because of the relatively lower cost and greater availability of gold compared to those of the platinum-group metals, supported Au nanocatalysts could potentially replace expensive platinum-group metal catalysts in such reactions. However, the direct applications of the supported Au nanocatalysts to the above industrial processes have been hampered by several problematic issues. One of the key issues is the stability of the gold nanocatalysts against sintering under reaction conditions. Accordingly, ultrastable supported Au nanocatalysts that are particularly impervious to high temperature treatments in an oxidizing atmosphere are extremely desirable to industrial applications because most of the above-mentioned reactions involve O<sub>2</sub> and proceed at high temperature.

One of the strategies in developing ultrastable supported Au nanocatalysts is to find a suitable substrate capable of efficiently stabilizing supported Au nanoparticles. For example, we have recently developed highly stable Au nanocatalysts supported on brookite nanoparticles.<sup>14</sup> Goodman and co-workers have reported the stabilization of highly active Au nanoparticles by surface defects via the substitution of Si with Ti in a silica thin film network.<sup>15</sup> Herein, we present another strategy for the preparation of ultrastable supported Au nanocatalysts by deposition of Au nanoparticles on a surface-modified nanocrystalline TiO<sub>2</sub>. The external surface of the nanocrystalline TiO<sub>2</sub> was modified by aluminum oxide via a surface sol–gel process (SSP).<sup>16,17</sup> The essence of this surface-modification technique is to allow the control of interfacial thickness and composition with molecular precision based on self-limiting surface reactions.<sup>16,17</sup>

The Au nanoparticles were deposited by a deposition–precipitation (DP) process<sup>2</sup> on the nanocrystalline TiO<sub>2</sub> whose surface was modified with Al<sub>2</sub>O<sub>3</sub> surface layers through SSP. The stabilization of Au nanoparticles was achieved through their interfacial interaction with the amorphous Al<sub>2</sub>O<sub>3</sub> surface layers. Such interaction was the key factor in giving rise to the ultrastable Au nanocatalysts that resisted sintering under high-temperature treatments. In sharp contrast, the Au nanoparticles supported on the corresponding unmodified-surface nanocrystalline TiO<sub>2</sub> showed very poor stability under identical treatments, as observed previously.<sup>1,2</sup>

The detailed information for the synthesis and characterization of the Au nanocatalysts as well as gold loadings is included in the Supporting Information. The calcination was carried out at 500 °C for 2.5 h in premixed 8% O<sub>2</sub>–He with a heating rate of 10 °C/min. Figure 1a compares the light-off curves of the as-synthesized gold catalyst supported on Degussa P25 TiO<sub>2</sub> with that for Al<sub>2</sub>O<sub>3</sub>-modified external surfaces (Au/Al<sub>2</sub>O<sub>3</sub>/P25). Figure 1b compares the same catalysts after calcination. Before calcination, these two

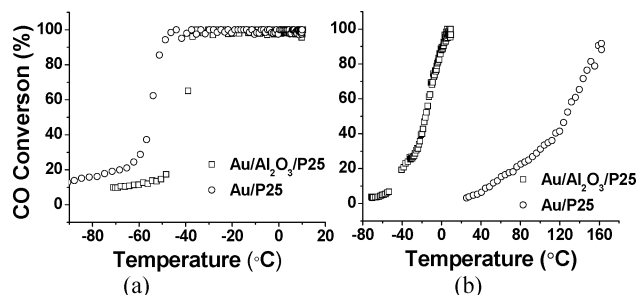
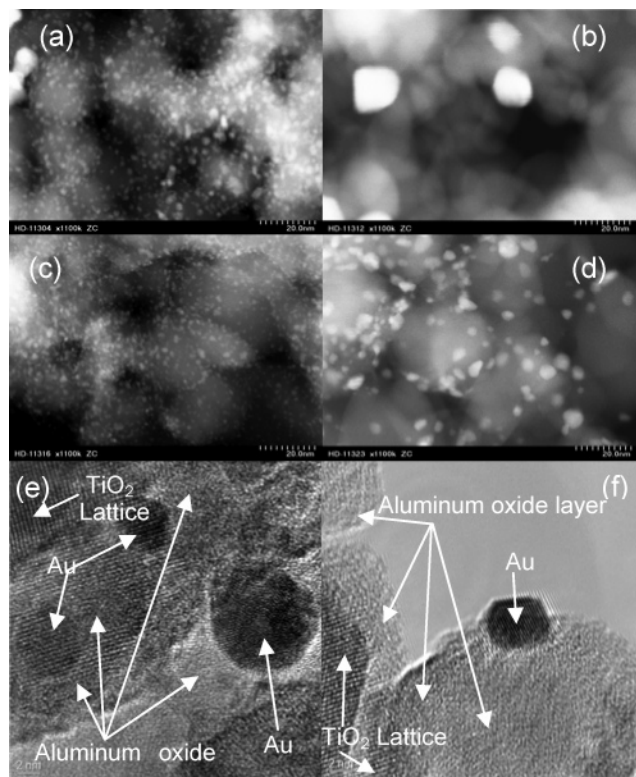


Figure 1. Light-off curves of as-synthesized (a) and calcined (b) Au/Al<sub>2</sub>O<sub>3</sub>/P25 and Au/P25.

as-synthesized catalysts were highly active for CO oxidation. Catalyst Au/P25 exhibited a higher activity with a  $T_{50}$ , the temperature at which 50% conversion of CO to CO<sub>2</sub> was achieved, as low as –55 °C. The  $T_{50}$  value for the Au/Al<sub>2</sub>O<sub>3</sub>/P25 was –40 °C. Even though both catalysts displayed a decreased activity after calcination, Au/Al<sub>2</sub>O<sub>3</sub>/P25 was still highly active and reached 50% CO conversion at a relatively low temperature of –17 °C. However, catalyst Au/P25 was considerably deactivated by calcination and reached 50% conversion at a much higher temperature of 125 °C. Clearly, the surface modification of the TiO<sub>2</sub> nanocrystals with aluminum oxide significantly improved the stability of the supported Au nanoparticles and had little effect on the gold loadings of the resulting catalyst supports through DP (see Supporting Information).

The TEM images of the as-synthesized and calcined Au/Al<sub>2</sub>O<sub>3</sub>/P25 and Au/P25 catalysts and high-resolution TEM (HRTEM) images of the as-synthesized and calcined Au/Al<sub>2</sub>O<sub>3</sub>/P25 catalyst are shown in Figure 2. The Z-contrast STEM images recorded at an identical magnification show that the as-synthesized Au/P25 [Figure 2a] and Au/Al<sub>2</sub>O<sub>3</sub>/P25 [Figure 2c] catalysts have a similar Au nanoparticle population and particle-size distribution. (For Au particle size distribution calculated from their TEM images, see Figure S3, Supporting Information.) The tiny, highly uniform bright spots (0.8–4.0 nm diameter) in Figure 2a,c correspond to the deposited gold precursor species. After calcination, Au nanoparticles supported by the surface-unmodified P25 showed significant sintering to form large Au particles presented in Figure 2b. The size of Au particles is generally greater than 5 nm and up to ~35 nm. (For additional TEM images taken at lower magnification, see Supporting Information.) However, the size of the Au nanoparticles supported on the surface-modified Al<sub>2</sub>O<sub>3</sub>/P25 support increased only slightly after the calcinations (generally in the 1–6 nm size range, see Figure 2d). The HRTEM images and EDX measurements of the as-synthesized Au/Al<sub>2</sub>O<sub>3</sub>/P25 catalyst [Figure 2e] revealed that the surface of TiO<sub>2</sub> was covered by amorphous aluminum-oxide layers and the Au nanoparticles were deposited on Al<sub>2</sub>O<sub>3</sub> amorphous layers (see the Supporting Information for additional HRTEM images). After calcination, the Au nanoparticles remained attached on the amorphous aluminum oxide layers with clearly visible lattice



**Figure 2.** Z-contrast TEM of as-synthesized (a) and calcined (b) Au/P25, as-synthesized, (c) and calcined (d) Au/Al<sub>2</sub>O<sub>3</sub>/P25 and HRTEM of as-synthesized (e) and calcined (f) Au/Al<sub>2</sub>O<sub>3</sub>/P25.

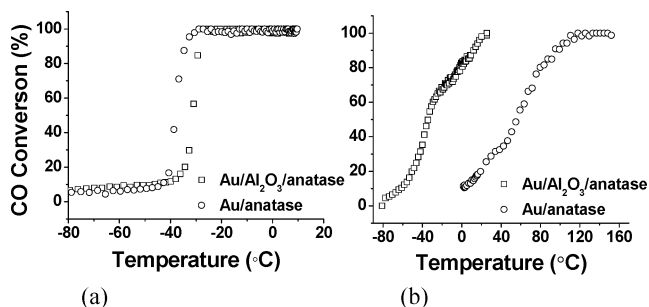


**Figure 3.** Light-off curves of (a) as-synthesized and (b) calcined Au/Al<sub>2</sub>O<sub>3</sub>/anatase and Au/anatase.

structure [Figure 2f], indicating the morphological transformation of the Au particles to the faceted nanocrystals. XRD analysis confirmed that there was no detectable crystalline alumina in the calcined catalyst, while ICP and EDX analysis (see Supporting Information) confirmed the existence of aluminum in the catalyst. This information strongly suggests that the amorphous aluminum-oxide layers play an extremely important role in the stabilization of the supported Au nanoparticles.

In addition to P25, which is a mixture of 70 wt % anatase and 30 wt % rutile, we have also modified the surface of pure anatase nanoparticles with aluminum oxide. Figure 3a compares the light-off curves of the as-synthesized Au/Al<sub>2</sub>O<sub>3</sub>/anatase with Au/anatase while Figure 3b compares these same catalysts after calcinations. As seen clearly from Figure 3, the surface-modified Au/Al<sub>2</sub>O<sub>3</sub>/anatase catalyst is considerably more stable against sintering than

the surface-unmodified Au/anatase catalyst, further supporting the importance of surface modification (see Supporting Information, Figure s1) for controlling catalyst stability. The light-off curves for the as-received and calcined reference gold catalysts supplied by the World Gold Council are included in Supporting Information for comparison purposes. For the latter catalyst, significant deactivation was also observed following calcination (Supporting Information Figure s2).

In summary, the surfaces of TiO<sub>2</sub> nanoparticles of P25 and anatase were modified with amorphous aluminum oxide using a surface sol-gel process. Ultrastable Au nanocatalysts were prepared by the deposition of Au nanoparticles on the surface-modified TiO<sub>2</sub> using a DP method. The TEM analysis showed that Au nanoparticles on the surface-modified supports were less susceptible to sintering during high-temperature calcination. The HRTEM analysis revealed that the surface of the TiO<sub>2</sub> nanoparticles was covered by an amorphous aluminum-oxide layer and the Au nanoparticles were primarily anchored to this amorphous layer. This amorphous aluminum-oxide layer played an extremely important role in the stabilization of the supported Au nanoparticles without affecting catalytic activities. The surface modification of nanocrystal supports can be a viable route to tailor the stability and activity of supported catalysis systems. The detailed structural mechanism for the enhanced stability is currently under investigation.

**Acknowledgment.** This work was conducted at the Oak Ridge National Laboratory and supported by Office of Basic Energy Sciences, U.S. Department of Energy, under Contract No. DE-AC05-00OR22725 with UT-Battelle, LLC. This research was supported in part by an appointment for W.Y. to the Postdoctoral Research Associates Program.

**Supporting Information Available:** The preparation of Au nanocatalyst, characterization methods, more HRTEM images for Au/Al<sub>2</sub>O<sub>3</sub>/P25, EDX spectra, and TEM images of as-synthesized and calcined Au/Al<sub>2</sub>O<sub>3</sub>/anatase. This material is available free of charge via the Internet at <http://pubs.acs.org>.

## References

- (1) Bond, G. C.; Thompson, D. T. *Catal. Rev.-Sci. Eng.* **1999**, *41*, 319.
- (2) Haruta, M. *CATTECH* **2002**, *6*, 102.
- (3) Hutchings, G. J. *Catal. Today* **2002**, *72*, 11.
- (4) Thompson, D. T. *Appl. Catal., A* **2003**, *243*, 201.
- (5) Hutchings, G. J. *Gold Bull.* **2004**, *37*, 3.
- (6) Moreau, F.; Bond, G. C.; Taylor, A. O. *J. Catal.* **2005**, *231*, 105.
- (7) (a) Guzman, J.; Gates, B. C. *J. Am. Chem. Soc.* **2004**, *126*, 2672. (b) Fu, Q.; Saltsburg, H.; Flytzani-Stephanopoulos, M. *Science* **2003**, *301*, 935.
- (8) Lin, S. D.; Bollinger, M.; Vannice, M. A. *Catal. Lett.* **1993**, *17*, 245.
- (9) (a) Calla, J. T.; Davis, R. J. *J. Phys. Chem. B* **2005**, *109*, 2307. (b) Kung, H. H.; Kung, M. C.; Costello, C. K. *J. Catal.* **2003**, *216*, 425.
- (10) Valden, M.; Lai, X.; Goodman, D. W. *Science* **1998**, *281*, 1647.
- (11) Schubert, M. M.; Hackenberg, S.; van Veen, A. C.; Muhler, M.; Plzak, V.; Behm, R. J. *J. Catal.* **2001**, *197*, 113.
- (12) (a) Arrii, S.; Morfin, F.; Renouprez, A. J.; Rousset, J. L. *J. Am. Chem. Soc.* **2004**, *126*, 1199. (b) Grunwaldt, J. D.; Kiener, C.; Wogerbauer, C.; Baiker, A. *J. Catal.* **1999**, *181*, 223.
- (13) (a) Cumarantunge, L.; Delgass, W. N. *J. Catal.* **2005**, *232*, 38. (b) Sinha, A. K.; Seelan, S.; Tsubota, S.; Haruta, M. *Angew. Chem., Int. Ed.* **2004**, *43*, 1546. (c) Yan, W. F.; Chen, B.; Mahurin, S. M.; Schwartz, V.; Mullins, D. R.; Lupini, A. R.; Pennycook, J.; Dai, S.; Overbury, S. H. *J. Phys. Chem. B* **2005**, *109*, 10676.
- (14) Yan, W. F.; Chen, B.; Mahurin, S. M.; Dai, S.; Overbury, S. H. *Chem. Commun.* **2004**, 1918.
- (15) Min, B. K.; Wallace, W. T.; Goodman, D. W. *J. Phys. Chem. B* **2004**, *108*, 14609.
- (16) Ichinose, I.; Senzu, H.; Kunitake, T. *Chem. Mater.* **1997**, *9*, 1296.
- (17) Yan, W. F.; Chen, B.; Mahurin, S. M.; Haganan, E. W.; Dai, S.; Overbury, S. H. *J. Phys. Chem. B* **2004**, *108*, 2793.

JA053191K